Stability of core-annular flow in a rotating pipe

Howard H. Hu and Daniel D. Joseph
Department of Aerospace Engineering and Mechanics, University of Minnesota, Minneapolis, Minnesota 55455

(Received 3 February 1989; accepted 16 June 1989)

The linear stability of core-annular flow in rotating pipes is analyzed. Attention is focused on the effects of rotating the pipe and the difference in density of the two fluids. Both axisymmetric and nonaxisymmetric disturbances are considered. Major effects of the viscosity ratio, interfacial tension, radius ratio, and Reynolds number are included. It is found that for two fluids of equal density the rotation of the pipe stabilizes the axisymmetric ($n = 0$) modes of disturbances and destabilizes the nonaxisymmetric modes. Except for small $\mathscr{R}$, where the axisymmetric capillary instability is dominant, the first azimuthal mode of disturbance $|n| = 1$ is the most unstable. When the heavier fluid is outside centripetal acceleration of the fluid in the rotating pipe is stabilizing; there exists a critical rotating speed above which the flow is stabilized against capillary instability for certain range of small $\mathscr{R}$. When the lighter fluid is outside the flow is always unstable.

I. INTRODUCTION

This paper is a further study on the linear stability of core-annular flow (CAF). In the previous works on the stability of CAF, Joseph, Renardy, and Renardy (JRR[1]), Preziosi, Chen, and Joseph (PCJ[2]), Hu and Joseph (HJ[3]), and recently Chen, Bai, and Joseph,[4] the pipe does not rotate. PCJ[2] and HJ[3] calculated growth rates and neutral curves. HJ[3] also carried out an energy analysis of small disturbances. By comparing with experiments, the linear theory can be correlated with the flow regimes that arise in practice: bubbles and slugs of oil and water, bubbly mixtures of oil and water, stable CAF, wavy core flow, and emulsions of water in oil. Flow regimes, wavelengths, and wave speeds seem to be predicted with fair accuracy by linear theory. This apparent success of the linear theory may eventually be shown to be fortuitous, but perhaps not more fortuitous than Rayleigh's celebrated criterion for the size of bubbles arising from capillary instability. In all the previous works it was found that the most unstable disturbance is axisymmetric ($n = 0$). In this paper we are going to study the situation of core-annular flow in a rotating pipe.

Linear stability theory for the rapid rotation of Poiseuille flow on one fluid in a pipe was studied by Pedley.[5,6] Joseph and Carmi[7] did a nonlinear energy analysis that applies to the same flow and found a nearly identical result (see Joseph[8]). They found that the flow is unstable to nonaxisymmetric disturbances for Reynolds number greater than 82.9. This instability has been confirmed for slow rotation both numerically and experimentally by Mackrodt.[9] Later, Cotton and Salwen[10] did extensive numerical computations on the problem. They all found the most unstable disturbance is nonaxisymmetric ($|n| = 1$).

II. BASIC FLOW

Consider two immiscible liquids flowing down a circular pipe in a concentric configuration with the inner layer (core) occupied by liquid 1 and outer layer (annulus) by liquid 2, the pipe is rotating with a constant angular velocity ω. The interface between the liquids is at $r = r_1(\theta,z,t)$, where (r,θ,z) are cylindrical coordinates and t is time. Let $\mathbf{U} = (u_r,u_\theta,u_z)$ be the velocity, $\hat{p}$ the pressure, μ_1, ρ_1 the viscosity and density of liquid 1, and μ_2 and ρ_2 the viscosity and density of liquid 2.

Assume that the pipe is infinitely long with axis at $r = 0$, the mean value of $r_1(\theta,z,t)$ over θ $(0 \leqslant \theta \leqslant 2\pi)$, and $z(-L \leqslant z \leqslant L, L \to \infty)$ is R_1, a constant that can be determined by prescribing the volume of each fluid in the linear theory of stability. We also assume that gravity can be neglected.

We scale the length with the pipe radius R_2, the velocity with the centerline velocity of basic flow W_0, pressure with $\rho_1 W_0^2$, time with R_2/W_0, and we use the same symbols for dimensional and dimensionless variables.

The basic flow with constant pressure gradient $\partial P/\partial z = -F$ and rigid rotation of the pipe is

$$\mathbf{U} = (0, V(r), W(r)) \text{ and } \hat{p} = P. \tag{1}$$

The tangential velocity is given by

$$V(r) = \epsilon r, \qquad r \in [0,1], \tag{2}$$

the axial velocity is given by

$$W(r) = \begin{cases} [1 - \eta^2 + m(\eta^2 - r^2)]/A, & r \in [0,\eta], \\ (1 - r^2)/A, & r \in [\eta,1], \end{cases} \tag{3}$$

and the pressure is determined by

$$\frac{\partial P}{\partial r} = \zeta_\prime [V^2(r)/r], \tag{4}$$

where $\zeta_\prime = 1$ or ζ corresponding to flows in the core or in the annulus,

$$A = 1 - \eta^2 + m\eta^2, \tag{5}$$

$$\eta = \frac{R_1}{R_2}, \quad m = \frac{\mu_2}{\mu_1}, \quad \zeta = \frac{\rho_2}{\rho_1}, \quad \epsilon = \frac{\omega R_2}{W_0}, \tag{6}$$

and the centerline velocity is given by

$$W_0 = (F/4\mu_2)(mR_1^2 + R_2^2 - R_1^2). \tag{7}$$

 0899-8213/89/101677-09$01.90

III. PERTURBATION EQUATIONS AND NORMAL MODES

We perturb the core-annular flow by writing (u,v,w,p) for the perturbations in the velocities and pressure and δ for the perturbation in the interface radius, and we introduce the dimensionless parameters

$$\mathscr{R} = \rho_1 W_0 R_2/\mu_1, \quad J^* = TR_2\rho_1/\mu_1^2, \tag{8}$$

where T is the coefficient of interfacial tension.

We use the normal mode decomposition of solutions:

$$[u,v,w,p](r,\theta,z,t) = [iu,v,w,p](r)\exp[in\theta + i\beta(z-ct)]$$

and

$$\delta(\theta,z,t) = \delta\exp[in\theta + i\beta(z-ct)], \tag{9}$$

where $u(r)$, $v(r)$, $w(r)$, and $p(r)$ are complex-valued functions and δ is a complex constant.

The linearized equations of motion are

$$\zeta_\ell\{[\beta(W-c)+n\epsilon]u + 2\epsilon v\} = p' - \frac{im_\ell}{\mathscr{R}}\left[\frac{d}{dr}\left(\frac{d}{r\,dr}(ru)\right) - \left(\beta^2 + \frac{n^2}{r^2}\right)u - \frac{2n}{r^2}v\right], \tag{10}$$

$$\zeta_\ell\{[\beta(W-c)+n\epsilon]v + 2\epsilon u\} = -\frac{n}{r}p - \frac{im_\ell}{\mathscr{R}}\left[\frac{d}{dr}\left(\frac{d}{r\,dr}(rv)\right) - \left(\beta^2 + \frac{n^2}{r^2}\right)v - \frac{2n}{r^2}u\right], \tag{11}$$

$$\zeta_\ell\{[\beta(W-c)+n\epsilon]w + W'u\} = -\beta p - \frac{im_\ell}{\mathscr{R}}\left[\frac{1}{r}\frac{d}{dr}\left(r\frac{dw}{dr}\right) - \left(\beta^2 + \frac{n^2}{r^2}\right)w\right], \tag{12}$$

$$\frac{d}{r\,dr}(ru) + \frac{n}{r}v + \beta w = 0, \tag{13}$$

where $W' = dW/dr$, $m_\ell = (1,m)$, $\zeta_\ell = (1,\zeta)$, $\ell = 1,2$ indicates the flow in core and in annulus.

The boundary conditions are

$$u = v = w = 0 \quad \text{at } r = 1, \tag{14}$$

u,v,w,p, and their derivatives

are finite at $r = 0$. (15)

The linearized interface conditions at $r = \eta$ are

$$u(\eta) = [\beta(W-c)+n\epsilon]\delta, \tag{16}$$

$$[u] = [v] = 0, \tag{17}$$

$$[w] + [W']\delta = 0, \tag{18}$$

$$[m_\ell(-\beta u + w')] = 0, \tag{19}$$

$$[m_\ell(-(nu+v)/r + v')] = 0, \tag{20}$$

$$[p] - (2i/\mathscr{R})[m_\ell u'] = -[\epsilon^2\eta(1-\zeta) + (J^*/\mathscr{R}^2\eta^2) \times (1-n^2-\eta^2\beta^2)]\delta, \tag{21}$$

where $[\ ] = (\ )_1 - (\ )_2$ is jump across $r = \eta$.

When we compare with the work of HJ,[3] where the rigid rotation of the pipe was not considered, we see that the differences of the linearized equations and interfacial conditions are as follows: all $\beta(W-c)$ in HJ[3] are to be replaced by $\beta(W-c)+n\epsilon$; there are two more terms in (10) and (11), $2\epsilon v$ and $2\epsilon u$, which couple the variables u and v; and there is an additional term $\epsilon^2\eta(1-\zeta)$ in the interfacial condition (21) resulting from the rotation of the pipe times the density difference of the fluids.

IV. ENERGY ANALYSIS

The linearized energy equation is obtained by multiplying (10), (11), and (12) by u_*, v_*, and w_*, the complex conjugates of u, v, and w, and integrating the sum of these three equations over $r = [0,1]$, exactly as in HJ.[3] The energy balance equation is

$$\dot{E} = I - D + B, \tag{22}$$

where

$$\dot{E} = \beta c_i \sum_{\ell=1}^{2}\int_{\Omega_\ell}\zeta_\ell(u^2+v^2+w^2)r\,dr,$$

$$I = \sum_{\ell=1}^{2}\int_{\Omega_\ell}\zeta_\ell W'\mathrm{Im}\{uw_*\}r\,dr,$$

$$D = \frac{1}{\mathscr{R}}\sum_{\ell=1}^{2}\int_{\Omega_\ell} m_\ell\left[\left(\frac{d(ru)}{rdr}\right)^2 + \left(\frac{d(rv)}{rdr}\right)^2 + \left(\frac{dw}{dr}\right)^2 + \left(\beta^2+\frac{n^2}{r^2}\right)(u^2+v^2+w^2) + \frac{4n}{r^2}\mathrm{Re}\{uv_*\}\right]r\,dr + \frac{1}{\mathscr{R}}(u_{(0)}^2 + v_{(0)}^2), \tag{23}$$

$$B = \mathrm{Im}\left\{\left[-pru_* + \frac{i}{\mathscr{R}}m_\ell\left(\frac{d(ru)}{rdr}ru_* + \frac{d(rv)}{rdr}rv_* + \frac{dw}{dr}rw_*\right)\right]\right\},$$

where $\Omega_1 = [0,\eta)$, $\Omega_2 = (\eta,1]$, and $u^2 = u\cdot u_*$, $v^2 = v\cdot v_*$,.... Here $\dot{E}$ is the rate of change of kinetic energy of the perturbed flow, I is the rate at which energy is transferred from the basic flow to the perturbed flow through the Reynolds stress, $-D$ is the rate of viscous dissipation of the perturbed flow, and B is the rate at which energy is being supplied at the interface.

In this case, the interfacial energy B can be written as

$$B = B1 + B2 + B3, \tag{24}$$

where

$$B1 = (\beta c_i)\frac{J^*}{\beta^2\mathscr{R}^2}\frac{1-n^2-\eta^2\beta^2}{\eta|W(\eta)-c+n\epsilon/\beta|^2}u^2(\eta),$$

$$B2 = \frac{2(1-m)}{\mathscr{R}}\left[v^2(\eta) - \mathrm{Re}\left(\eta u'(\eta^+)u_*(\eta) + \frac{\eta^2(2-m)}{A|W(\eta)-c+n\epsilon/\beta|}u^2(\eta) + \frac{\eta^2 m}{A\beta|W(\eta)-c+n\epsilon/\beta|_*}w'(\eta^+)u_*(\eta)\right)\right] \tag{25}$$

and

$$B3 = (\beta c_i)\frac{\epsilon^2\eta^2(1-\zeta)}{\beta^2|W(\eta)-c+n\epsilon/\beta|^2}u^2(\eta).$$

The interfacial energy $B1$ is due to surface tension, $B2$ is due to the difference of viscosity of two fluids, and the new term $B3$ is due to the difference of density of two fluids and the rotation of the pipe. Obviously if $\zeta > 1$ (the heavier fluid is centrifuged), this new term $B3$ is stabilizing ($B3 < 0$), while if $\zeta < 1$ (the lighter fluid is in annulus), $B3$ is a destabilizing ($B3 > 0$).

Since the amplitude of velocities u, v, w (or eigenfunctions) is arbitrary, the value of each term of energy is normalized with $D = 1$.

V. NUMERICAL METHOD

Following HJ,[3] the coupled eigenvalue equations (10)–(13) with boundary and interface conditions (14)–(21) are solved using a finite element method. We again take the Hermite polynomials as the interpolation functions for u and the Lagrange polynomials for v, since the governing equation for u after eliminating w is fourth order while the equation for v is second order.

After discretization, we obtain an eigenvalue system

$$\mathbf{Ax} = (c - n\epsilon/\beta)\mathbf{Bx}, \tag{26}$$

where $c = c_r + ic_i$ is an eigenvalue introduced in (9), $\mathbf{A}$ and $\mathbf{B}$ are the global matrices and

$$\mathbf{x} = \left[u_1, \left(\frac{du}{dr}\right)_1, v_1, u_2, \left(\frac{du}{dr}\right)_2, v_2, \ldots, u_N, \left(\frac{du}{dr}\right)_N, v_N\right]^T,$$

N is the total number of nodes.

The eigensystem (26) is solved with the IMSL routine EIGZC on the Cray 2.

Since $r = 0$ is a singular point, precaution for the integrations over the first element is needed. We find this especially important for the cases in which ϵ is large. We did the exact integration over $[r,\Delta]$ for the first elemental matrices, where Δ is the length of the first element and r tends to zero. In this way we also find the proper boundary conditions at origin, which are the same as those derived in PCJ.[2]

Equations (10)–(13) with conditions (14)–(21) show that we cover all possibilities when increasing z is the direction of flow and $\mathscr{R} > 0$ while the parameters (ϵ,n,β) can be either positive or negative. To determine the symmetries of these equations we change ϵ to $-\epsilon$, n to $-n$ and v to $-v$ and verify that Eqs. (10)–(21) are unchanged. This symmetry implies that the growth rate βc_i is unchanged under the change of these signs, or changing ϵ to $-\epsilon$ is equivalent to changing n to $-n$. Similarly, if we take the complex conjugates of these equations and conditions, we find that changing n to $-n$ is equivalent to changing β to $-\beta$; therefore changing the sign of any two of the three parameters (ϵ,n,β) leaves the growth rate βc_i invariant. This argument shows that all cases are realized in the set of $\mathscr{R} \geqslant 0$, $n \geqslant 0$, $\epsilon \geqslant 0$, and $\beta \in [-\infty, \infty]$. If either $n = 0$ or $\epsilon = 0$, all possible growth rates are contained in a set of parameters in which $\beta \geqslant 0$.

In our computation a new parameter

$$\Omega = \epsilon\mathscr{R} = \rho_1 \omega R_2^2/\mu_1 \tag{27}$$

is introduced. This parameter can be more easily controlled in experiments than ϵ.

For the results given in this paper, 30 elements are used (15 in core + 15 in annulus). The size of the element is not uniform; smaller elements are used for regions near the pipe wall and the interface, taking into account effects of the boundary layer in these regions. In some cases 25 + 25 elements were used to check our results. The results were almost the same.

As a further check of our code we compared our results with some neutral stability data given in Cotton and Salwen[10] (Table I) for rotating Hagen–Poiseuille flow of one fluid, the comparison is listed in Table I. The results for low $\mathscr{R}$ are almost the same; for high $\mathscr{R}$ our results are slightly lower than theirs but the discrepancy is within 1.8%. Thus we are confident about our code.

VI. $\zeta = 1$, TWO FLUIDS OF EQUAL DENSITY

In this paper, we consider the case $m < 1$, a viscous core with lubricating annulus, for example, an oil core with water annulus. As a typical situation we choose parameters $J^* = 1000$, $\eta = 0.8$, and $m = 0.1$ and basically study the effects of Ω (rotational speed), ζ (the density ratio), and n (the azimuthal wavenumber). Results exhibited in the papers of JRR,[1] PCJ,[2] and HJ[3] show that for $\Omega = 0$ the axisymmetric disturbances of core-annular flow are most dangerous. On the other hand, the most unstable disturbance of the rotating Poiseuille flow of one fluid is not axisymmetric and has a $n = 1$ azimuthal periodicity. In this paper we studied both modes, $n = 0$ and $n = 1$. We find that when $\Omega \neq 0$, $n = 1$ is especially important.

First we consider the case of $\zeta = 1$; the two fluids have the same density.

Figure 1 presents the neutral curves for $J^* = 1000$, $\eta = 0.8$, $m = 0.1$, and $n = 0$ with $\Omega = 0$, 50, 100, and 200. When $\Omega = 0$, the neutral curve has nicely separated upper branch and lower branch, typical for CAF. We see clearly that the rotation of the pipe stabilizes the upper branch (lifts the branch higher). The effect of rotation on the lower branch depends on the value of Ω: for small Ω, the rotation compresses the unstable region in the bottom left-hand corner, so it is stabilizing; as Ω increases, this margin of stability is raised and the rotation is destabilizing. This shows that fast rotation can supress the effects of shear stabilization of capillary instability. It is in this range of Ω that we find $n = 0$

TABLE I. Comparison of neutral stability data with data given by Cotton and Salwen[10] for rotating Hagen–Poiseuille flow of one fluid, when n, β, and Ω are given and $\mathscr{R}$ corresponding to neutral stability is computed.

n	β	Ω	$\mathscr{R}$ in Ref. 10	$\mathscr{R}$ (present result)
1	−0.1	415	83.1	83.11
1	−1.0	51.8	109	109.3
1	−2.0	835	2810	2791
2	−0.1	909	91.2	91.37
2	−1.0	106	108	107.7
2	−2.0	972	1840	1808
3	−0.1	1650	110	110.5
3	−1.0	186	125	124.8
3	−2.0	1560	2020	1995
5	−1.0	438	176	175.7
10	−1.0	1780	356	356.5
15	−1.0	4500	600	600.5
30	−1.0	25 100	1680	1681.3

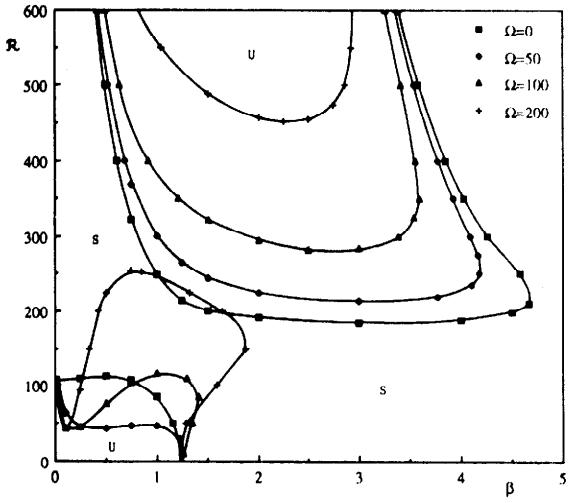

FIG. 1. Neutral curves for the axisymmetric mode ($n = 0$) when two fluids are of equal density $\zeta = 1$. Increasing the rotational speed Ω of the pipe stabilizes the upper branch and at first stabilizes, then destabilizes, the lower branch. ■: $\Omega = 0$; ◆: $\Omega = 50$; △: $\Omega = 100$; +: $\Omega = 200$.

is not the most unstable mode; the $n = 1$ mode comes into play.

In Fig. 2 we have displayed the neutral curves for $n = 1$ with parameters at the values set in Fig. 1 together with the neutral curves for $n = 0$ for comparison. We see that for $\Omega = 0$ the neutral curve in the $(\mathscr{R}, -\beta)$ plane is just the reflection of the curve in the $(\mathscr{R},\beta)$ plane. This symmetry was established by the argument given in Sec. V. The neutral curve for $n = 1$ lies within the curve for $n = 0$, so $n = 0$ is more unstable in this case, a result that we obtained in previous papers. As Ω increases, the neutral curve for $n = 1$ loses symmetry with respect to β. For positive β the neutral curve $\mathscr{R}(\beta)$ moves up as Ω increases; while for negative β the upper branch of neutral curve moves down (destabilizing the flow) as Ω increases.

In Fig. 2 we cannot see clearly how the neutral curve for the $n = 1$ mode moves as Ω increases, so we present curves for $\Omega = 0$, 10, 25, and 50 in Fig. 3. From this figure it is clear how asymmetry develops as Ω increases.

Actually $\Omega = 50$ is not a big number. Consider an experiment with oil and water. Assume that the viscosity ratio is

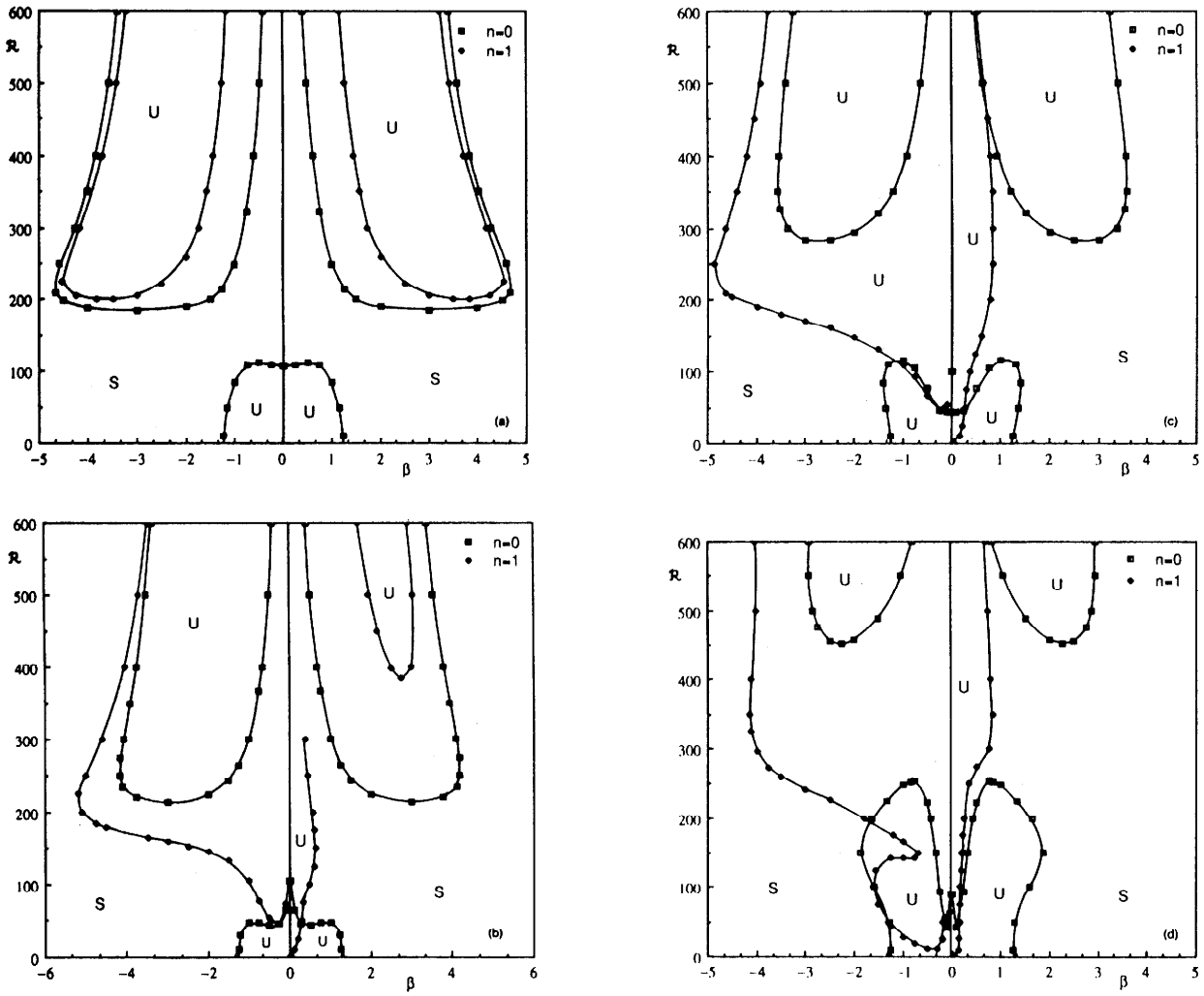

FIG. 2. Neutral curves for the first mode of azimuthal periodicity ($n = 1$) compared with the neutral curves for the asymmetric mode ($n = 0$). (a) $\Omega = 0$; (b) $\Omega = 50$; (c) $\Omega = 100$; and (d) $\Omega = 200$. At $\Omega = 50$, $n = 1$ is more unstable at left plane ($-\beta$ plane). ■: $n = 0$; ◆: $n = 1$.

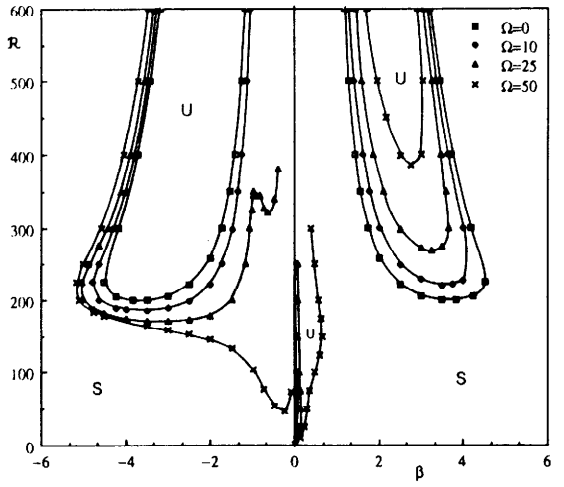

FIG. 3. Neutral curves for disturbance with $n = 1$ when Ω is from 0–50. This figure clearly shows how the curves move when Ω increases. ■: $\Omega = 0$; ◆: $\Omega = 10$; △: $\Omega = 25$; ×: $\Omega = 50$.

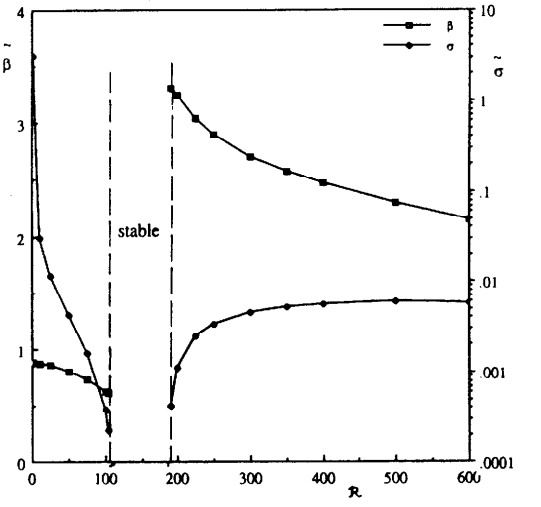

FIG. 4. The wavenumber $\tilde{\beta}$ of maximum growth and the corresponding growth rate $\tilde{\sigma}$ as a function of $\mathscr{R}$ when $\Omega = 0$. ■: $\tilde{\beta}$; ◆: $\tilde{\sigma}$.

$\mu_{\text{water}}/\mu_{\text{oil}} = 0.1$, density is nearly matched and the diameter of the pipe is 1 in., then

$$\Omega = \rho_{\text{oil}}\omega R^2/\mu_{\text{oil}} = 14.2\omega.$$

$\Omega = 50$ corresponds to $\omega = 3.5\ \text{sec}^{-1}$ or 33.7 rpm, the rotating speed is not too fast.

If we examine Figs. 2 and 3 more carefully, we see that for negative β the neutral curve for $n = 1$ has a valley near $\beta = 0$. This valley is related to another mode of instability, interfacial friction associated with the viscosity difference. This will be clear when we study the energy budget. We also note that there is a small unstable region $\beta > 0$ near $\beta = 0$, this is also associated with instability resulting from interfacial friction; the growth rates in this region are smaller than those either in the unstable region of the $(\mathscr{R}, -\beta)$ when $n = 1$ or those in the unstable region when $\mathscr{R}$ is small and $n = 0$. These changes of the neutral curves with Ω show that rotation of the pipe induces instability because of interfacial friction.

Figure 4 shows the variation of wavenumber $\tilde{\beta}$ of maximum growth and corresponding growth rate $\tilde{\sigma} = \tilde{\beta} c_i(\tilde{\beta})$ with Reynolds number $\mathscr{R}$ for $\Omega = 0$. There is a stable region corresponding to the gap between the upper branch and lower branch of the neutral curve.

Figures 5 and 6 present the maximum growth rate $\tilde{\sigma}$ and corresponding wavenumber $\tilde{\beta}$ for $\Omega = 50$ and 200, respectively. Since changing the sign of n is equivalent to changing the sign of β, we may restrict our attention to $\beta > 0$ and change the sign of n. It is clear that except for small $\mathscr{R}$, where the growth rate $\tilde{\sigma}$ for $n = 0$ is larger, the $n = -1$ mode is always more unstable. The regions that are stable to axisymmetric disturbances are destabilized by the azimuthal mode with $n = -1$. We also draw attention to the jump in the curves in Figs. 5(b) and 6(b) at $\mathscr{R}$ about 90. This jump is associated with a switch in the mode of disturbance, which is most destabilizing.

We know for HJ[3] that the energy analysis for small perturbances is very useful in this situation; it helps to diagnose

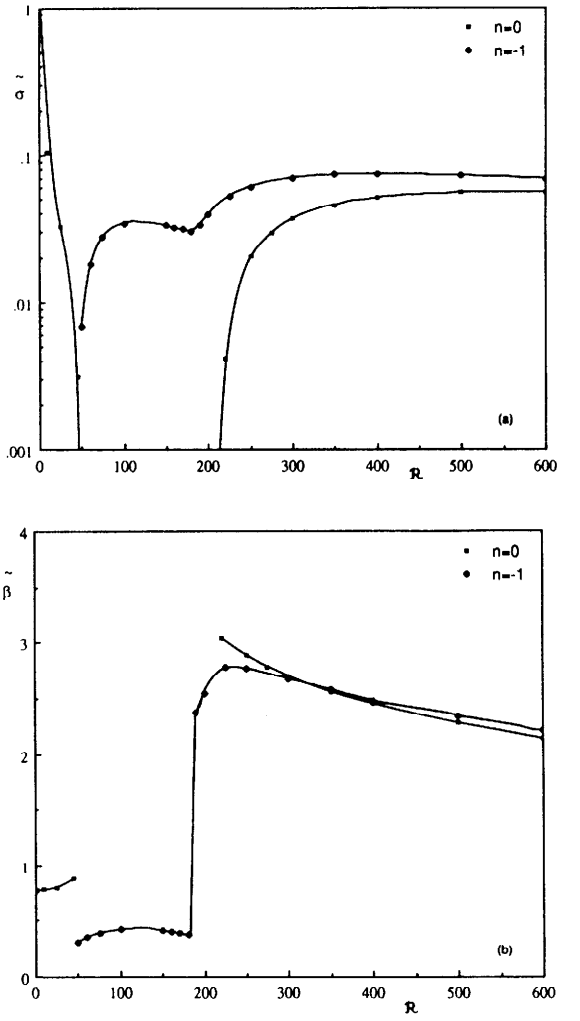

FIG. 5. The maximum growth rate $\tilde{\sigma}$ (a) and corresponding wavenumber $\tilde{\beta}$ (b) for $n = 0$ and $n = -1$ when $\Omega = 50$. The mode corresponding to $n = -1$ is more unstable than $n = 0$ when $\mathscr{R}$ is not too small. The wavenumber $\tilde{\beta}$ of the most dangerous disturbance with $n = -1$ jumps at a certain $\mathscr{R}$ because of a switch in the modes of most destabilizing. ■: $n = 0$; ◆: $n = -1$.

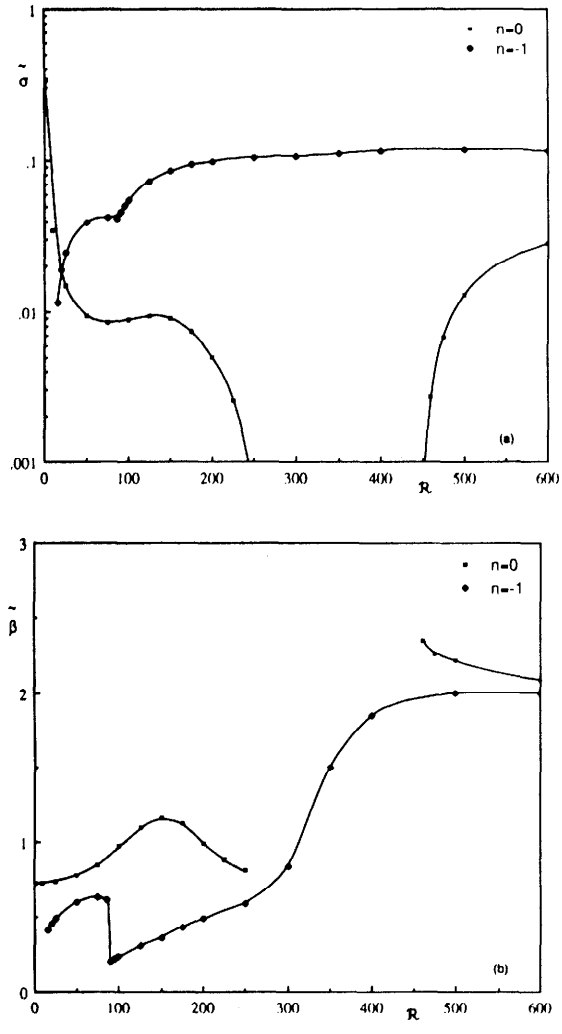

FIG. 6. The maximum growth rate σ (a) and corresponding wavenumber β (b) for $n = 0$ and $n = -1$ when $\Omega = 200$. ■: $n = 0$; ◆: $n = -1$.

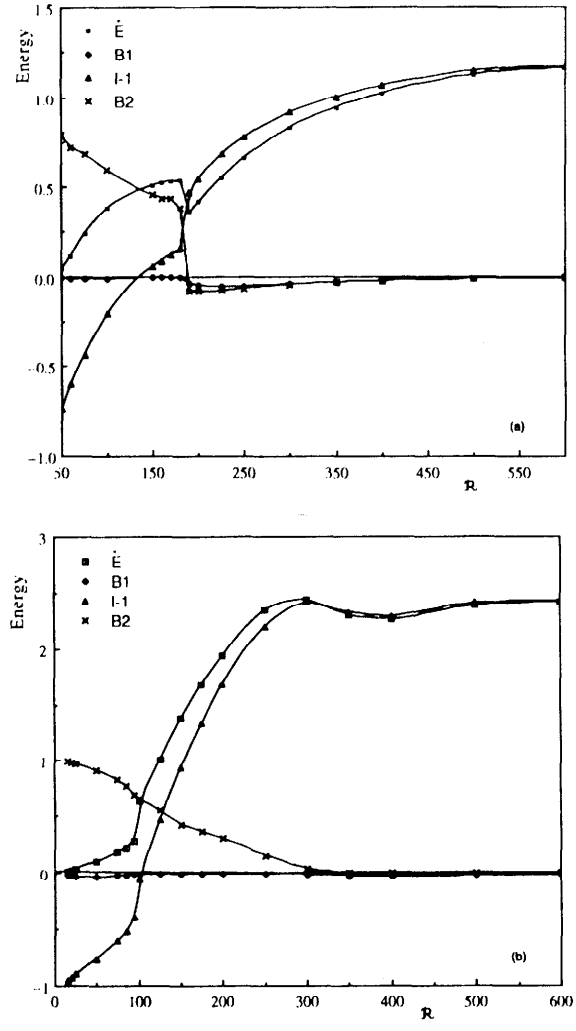

FIG. 7. Variation of terms of energy $\dot{E}$: ■; $B1$: ◆; $I-1$: △; and $B2$: × in the energy balance equation following the wavenumber of maximum growth for $n = -1$, (a) $\Omega = 50$ and (b) $\Omega = 200$.

the sources of instability. At small $\mathscr{R}$, we know that the flow is unstable to the $n = 0$ mode mainly because of the interfacial tension $B1$ producing capillary instability. In Fig. 7 we plotted each of the terms in the energy equation for $n = -1$ as a function of $\mathscr{R}$ when (a) $\Omega = 50$ and (b) $\Omega = 200$, at the wavenumber of maximum growth $\tilde{\beta}$. In the present case, since the fluids have the same density, $B3 = 0$, and the energy equation (22) reduces to

$$\dot{E} = (I - 1) + B1 + B2.$$

In Fig. 7(a) we see that $B1$ (interfacial tension) is almost zero for all $\mathscr{R}$; it does not play an important role here. The two main sources of instability are $(I - 1)$ and $B2$. At small $\mathscr{R}$ (not so small when $n = 0$ is the most unstable mode), interfacial friction $B2$ is dominant. Since we know from the comparison with experiments in HJ[1] that this interfacial friction instability correlates with interfacial waves, we might see spiral waves at the interface. As $\mathscr{R}$ is increased, $B2$ decreases but $I - 1$ increases. At a certain Reynolds number $B2$ has a sudden decrease and $I - 1$ has a sudden increase. This shows that the mode of instability jumps from interfacial friction to the Reynolds stress. At large $\mathscr{R}$, $I - 1$ dominates and the flow is unstable by virtue of the production of energy in the bulk fluid with negligible contributions from the interfacial terms $B1$ and $B2$. In many of the cases discussed in HJ[1] this instability profile correlates with observed flows in which small drops of water emulsify into oil. In Fig. 7(b) the decrease of $B2$ is quite gradual but the increase of $I - 1$ is still sharp at certain value of $\mathscr{R}$. This mode jump is different from the one in Fig. 7(a), it is just the switching between different modes of instability resulting from interfacial friction.

In this section we have seen that the rotation of the pipe stabilizes the $n = 0$ mode and destabilizes the $n = 1$ mode, except for small $\mathscr{R}$, where capillary instability is dominant. This means that if the pipe rotates, or perhaps if the flow has a small azimuthal component, the flow will be unstable to the $n = 1$ mode leading to spiral waves at interface instead of stable core annular flow.

VII. $\zeta > 1$, HEAVIER FLUID OUTSIDE

The configuration, with heavy fluid outside $\zeta > 1$, is stably stratified. The stabilizing effect of centripetal acceleration in this case was already shown in the energy analyses of Sec. IV, $B3 < 0$ (stabilizing) for $\zeta > 1$. Actually, even the problem of rigid rotation of two fluids without axial flow is very complicated and very nonlinear, with stability possible even with $\zeta < 1$, provided that the stable configuration is taken closer to a rotating drop than to a perfect circular annulus (see Joseph and Preziosi[11]).

Figures 8–10 present neutral curves for $\zeta = 1.2$, 2, and 10, respectively, where (a) is for $n = 0$ and (b) is for $n = -1$. First we consider the case $\Omega = 0$. As ζ increases, the upper branch of the neutral curve moves down to small $\mathscr{R}$ and the lower branch is depressed. The flow becomes increasingly prey to instability on the upper branch and is stabilized with respect to capillary instability on the lower branch by making the lubricating fluid heavier. From Fig.

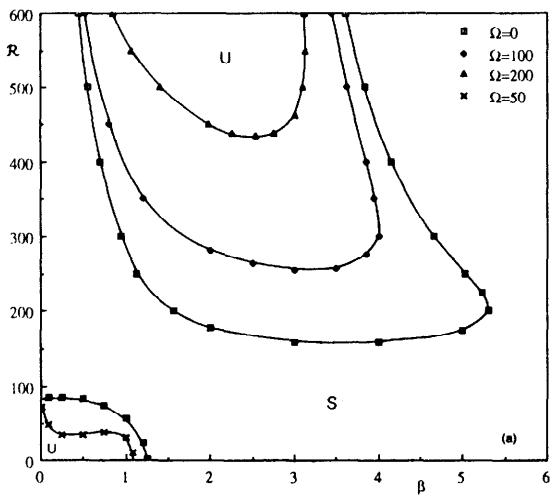

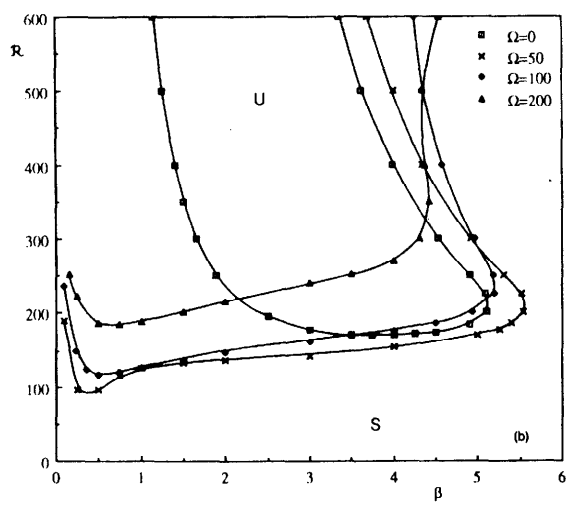

FIG. 8. Neutral curves for $\zeta = 1.2$ when $\Omega = 0$, 50, 100, and 200. (a) $n = 0$, (b) $n = -1$. Rotation of the pipe stabilizes the flow. For Ω other than 0, the $n = -1$ mode is more unstable. The upper branch of neutral curve for $\Omega = 50$ is not presented here. At $\Omega = 100$ the lower branch disappears, thus it is possible to have stable continuous CAF in certain range of small $\mathscr{R}$ if the rotating speed is large. ■: $\Omega = 0$; +: $\Omega = 50$; ◆: $\Omega = 100$; △: $\Omega = 200$.

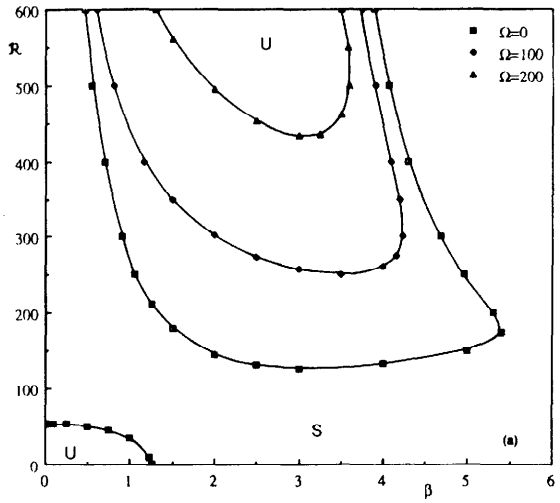

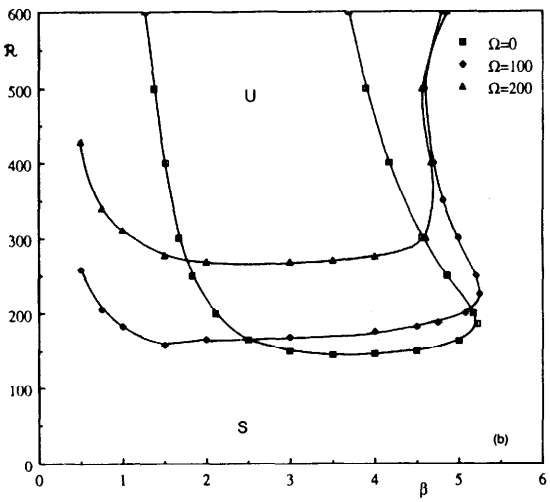

FIG. 9. Neutral curves for $\zeta = 2.0$ when $\Omega = 0$, 100, and 200. (a) $n = 0$, (b) $n = -1$. ■: $\Omega = 0$; ◆: $\Omega = 100$; △: $\Omega = 200$.

8(a), we see that the rotation of the pipe greatly lifts the upper branch of the curve (as we saw already in Fig. 1) and depresses the lower branch. Actually there exists a critical value $\Omega = \Omega_c$, above which there is no capillary instability (the lower branch of neutral curve disappears). We can determine this value of $\Omega = \Omega_c$ analytically as follows.

The energy balance $\dot{E} = (I - D) + B1 + B2 + B3$ is considered when $\mathscr{R} \ll 1$. We know that $\dot{E}$ and I are not related explicitly to $\mathscr{R}$, D and $B2$ are proportional to $1/\mathscr{R}$, and $B1$ and $B3$ are proportional to $1/\mathscr{R}^2$ (since in $B3$, $\epsilon = \Omega/\mathscr{R}$). Thus for $\mathscr{R} \ll 1$ we could neglect the lower-order terms and what is left is $B1 + B3$, interfacial tension plus the term that is proportional to the density difference.

Substituting (25) for $B1$ and $B3$, we have

$$B1 + B3 = (\beta c_i)\Delta(u^2(\eta)/\{\beta^2\mathscr{R}^2|W(\eta) - c + n\epsilon/\beta|^2\}), \tag{28}$$

where

$$\Delta = J^*(1 - n^2 - \eta^2\beta^2)/\eta - \Omega^2\eta^2(\zeta - 1). \tag{29}$$

Thus we know that for $\mathscr{R} \ll 1$ if $\Delta > 0$ flow is unstable (capil-

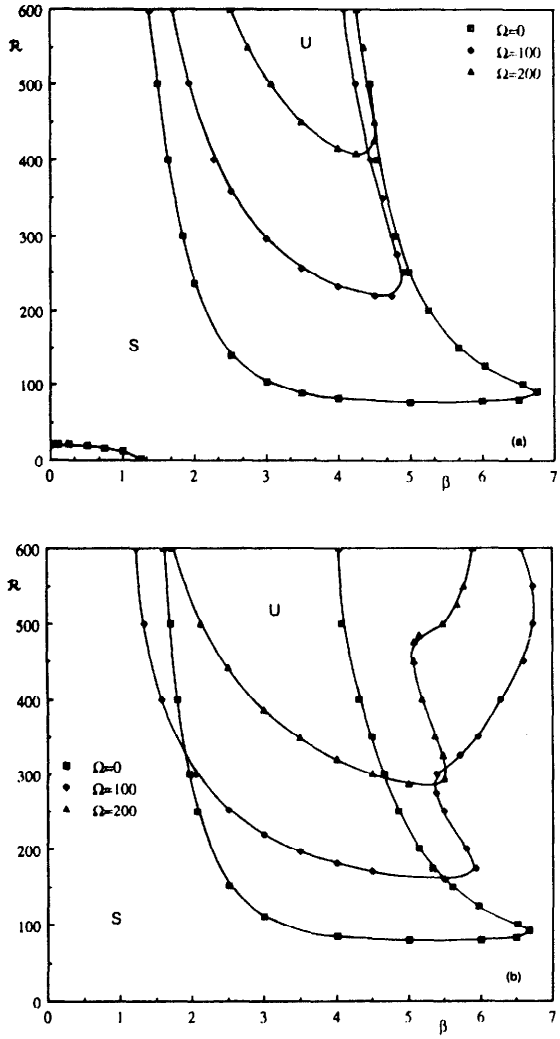

FIG. 10. Neutral curves for $\zeta = 10.0$ when $\Omega = 0$, 100, and 200. (a) $n = 0$, (b) $n = -1$. ■: $\Omega = 0$; ◆: $\Omega = 100$; △: $\Omega = 200$.

lary instability), and if $\Delta < 0$ CAF is stable, at neutral state $\Delta = 0$, that is

$$\Omega^2 = J^*(1 - n^2 - \eta^2\beta^2)/\eta^3(\zeta - 1). \tag{30}$$

Therefore

$$\Omega_c^2 = J^*(1 - n^2)/\eta^3(\zeta - 1). \tag{31}$$

We see that for $|n| > 1$ the flow is always stable to capillary instability, for $n = 0$ there exists a critical rotating speed of the pipe Ω_c above which the flow is stable to capillary instability. In the cases we presented in Figs. 8–10, $\Omega_c(\zeta = 1.2) = 98.8$, $\Omega_c(\zeta = 2) = 44.2$, and $\Omega_c(\zeta = 10) = 14.7$.

In Fig. 8(a) we plotted the lower branch of the neutral curve for $\Omega = 50$, we see that the lower branch starts at $\beta = 1.078$, as predicted in (30), and at other values of Ω this branch disappears.

Now look at Figs. 8(b), 9(b), and 10(b) in which $\zeta > 1$, comparing with the neutral curves for $\zeta = 1$ presented in Fig. 2(b)–(d). When $\zeta > 1$ the effect of increasing Ω is stabilizing, the upper branch of the neutral curves is raised. It is important to notice that for Ω other than zero, the neutral curves for $n = 0$ lie within the corresponding neutral curves for $n = -1$. This implies that when $\zeta > 1$ and $\Omega > 0$ the first azimuthal mode $n = -1$ is most dangerous.

Therefore, when the heavier fluid is outside, and $\Omega > \Omega_c$, stable continuous CAF is possible for a certain range of small $\mathscr{R}$ because of the stabilizing effects of rotation.

VIII. $\zeta < 1$, LIGHTER FLUID OUTSIDE

When the fluid in the annulus is lighter, $\zeta < 1$. Energy analysis then shows that the new term $B3$ is destabilizing. We call this centripetal instability, the centripetal acceleration throws heavier fluid in core outward. We shall see that this arrangement of fluids is alway unstable, as in Rayleigh–Taylor instability, when heavy fluid is above.

Figures 11 and 12 show neutral curves for $\zeta = 0.8$ and 0.5 with $\Omega = 0$, 100, and 200. The flow is always unstable to the $n = -1$ mode when Ω is not zero. At small $\mathscr{R}$, the flow is unstable to the $n = 0$ mode as is the case when $\zeta = 1$. At large $\mathscr{R}$, the $n = -1$ mode is more unstable. When $n = 0$

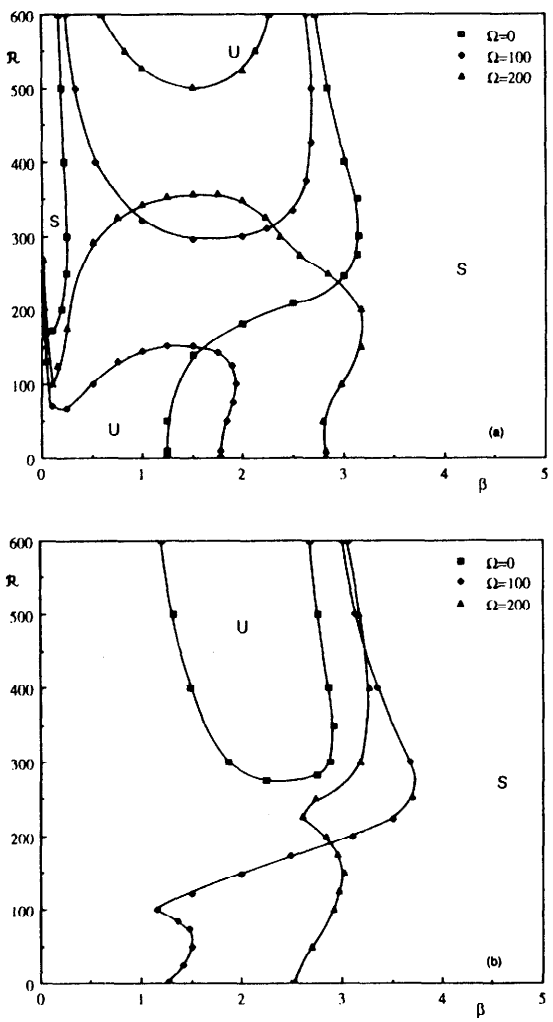

FIG. 11. Neutral curves for $\zeta = 0.8$ when $\Omega = 0$, 100, and 200. (a) $n = 0$, (b) $n = -1$. The flow is always unstable. At $\mathscr{R} \ll 1$, $n = 0$ mode is unstable to interfacial tension $B1$ and centripetal $B3$ instabilities; $n = -1$ mode is solely unstable to the centripetal instability $B3$. At high $\mathscr{R}$, $n = -1$ is more unstable than $n = 0$ mode. ■: $\Omega = 0$; ◆: $\Omega = 100$; △: $\Omega = 200$.

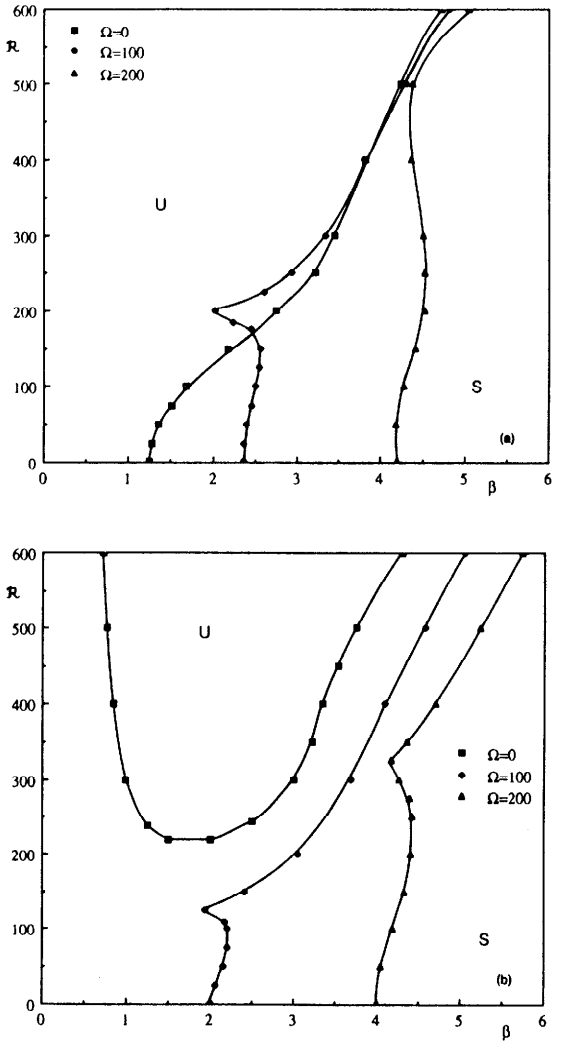

FIG. 12. Neutral curves for $\zeta = 0.5$ when $\Omega = 0$, 100, and 200. (a) $n = 0$, (b) $n = -1$. ■: $\Omega = 0$; ◆: $\Omega = 100$; Δ: $\Omega = 200$.

and $\Omega = 0$, the upper and lower branch of neutral curve join and no stable region exists. Rotation of the pipe lifts the upper branch (cf. Fig. 1). Fig. 11(a) shows that there is a stable region when Ω is large. As Ω increases or ζ decreases, the term $B3$ associated with centripetal instability increases and the unstable region enclosed in the lower part of neutral curve grows. This leads to the situation shown in Fig. 12(a) in which the interval of stability has disappeared. When $\mathscr{R} \ll 1$, following our discussion in Sec. VII, we find again using (29), that Δ is always positive for small β (long waves) when $n = 0$. Thus at small $\mathscr{R}$ when $n = 0$, there are two sources of instability, interfacial tension ($B1$) and the centripetal instability ($B3$). When $n \neq 0$ the only source of instability is the centripetal instability resulting from $B3$. Interfacial tension $B1$ leads to stability and there exists a critical rotational speed Ω_c given by (31), below which CAF is stable. At large $\mathscr{R}$, instability is due to the Reynolds stress. The sharp corners of the neutral curves in Fig. 11(b) and Fig. 12(b) are the result of mode switching between centripetal instability to Reynolds stress instability.

IX. CONCLUSIONS

In this paper we have studied the linear stability of core-annular flow in a rotating pipe emphasizing the effects of rotation and the difference in the density of two fluids.

For two fluids of equal density, rotation stabilizes the axisymmetric ($n = 0$) mode and destabilizes the nonaxisymmetric ($|n| = 1$) mode. Except for small $\mathscr{R}$, where capillary instability is dominant, the azimuthal mode $n = 1$ is the most unstable. With even rather slow rotation the flow will be unstable to the $n = 1$ mode. In this case we may observe spiral waves at interface instead of stable core-annular flow. In fact, we have observed such spiral waves in nonlinear regimes of wavy core flow in which shearing stresses give rise to a turning torque.

If the heavier fluid is outside, the rotation of the pipe stabilizes the flow, and there exists a critical rotating speed Ω_c, above which the flow is stable for certain range of small $\mathscr{R}$. If the lighter fluid is outside the flow is always unstable.

ACKNOWLEDGMENTS

This work was supported by the Army Research Office, Mathematics, the Department of Energy, and the National Science Foundation. Computer results were obtained under grants from the Academic Computing Services and Systems of the University of Minnesota, and from Minnesota Supercomputer Center.

[1] D. D. Joseph, Y. Renardy, and M. Renardy, J. Fluid Mech. **141**, 309 (1984).
[2] L. Preziosi, K. Chen, and D. D. Joseph, J. Fluid Mech. **201**, 323 (1989).
[3] H. H. Hu and D. D. Joseph, J. Fluid Mech. **205**, 359 (1989).
[4] K. Chen, R. Bai, and D. D. Joseph, submitted to J. Fluid Mech.
[5] T. J. Pedley, J. Fluid Mech. **31**, 603 (1968).
[6] T. J. Pedley, J. Fluid Mech. **35**, 97 (1969).
[7] D. D. Joseph and S. Carmi, Q. Appl. Math. **XXVI**(4), 576 (1969).
[8] D. D. Joseph, *Stability of Fluid Motion* (Springer, Berlin, 1976), Vol. 2, Sec. 46.
[9] P. A. Mackrodt, J. Fluid Mech. **73**, 153 (1976).
[10] F. W. Cotton and H. Salwen, J. Fluid Mech. **108**, 101 (1981).
[11] D. D. Joseph and L. Preziosi, J. Fluid Mech. **185**, 323 (1987).